



Mechanisms involved in thermal degradation of lignocellulosic fibers: a survey based on chemical composition

Heitor L. Ornaghi Jr. · Felipe G. Ornaghi · Roberta M. Neves · Francisco Monticeli · Otávio Bianchi

Received: 23 October 2019 / Accepted: 31 March 2020 / Published online: 9 April 2020
© Springer Nature B.V. 2020

Abstract The aim of this study was to determine the Arrhenius parameters and degradation mechanism for each component of biomass, including extractives, water, hemicellulose, cellulose and lignin. A statistical tool (F-test) was used as well as simulations of the effects of each component and the respective chars formed during thermal degradation. Experimental and theoretical curves for each component were simultaneously fitted, and the influence on the final thermal degradation curve was evaluated. Simulation of the TG curve was based on recently published models, for which one, two and three-step mechanisms were tested to complete the statistical evaluation. The activation energy showed a dependence on the cellulose and the reaction order on the hemicellulose polymer

structures. On the other hand, lignin is the most complex material in biomass and thus a broader range of degradation mechanisms is associated with its char and this plays a significant role in the final “tail” of the TG curve. In the case of cellulose and hemicellulose, autocatalysis is the most probable degradation mechanism while for the respective chars it is diffusion. The char formation significantly increases the activation energy. The results of this study provide an insight into the chemistry involved in the pyrolysis of multicomponent biomass, which will facilitate the building of a prediction model.

Keywords Modeling and simulation · Lignocellulosic · Thermal decomposition · Pyrolysis · Model-fitting

H. L. Ornaghi Jr. (✉) · F. Monticeli
Department of Materials and Technology, Fatigue and Aeronautic Materials Research Group, School of Engineering, Sao Paulo State University (UNESP), Guaratinguetá, SP, Brazil
e-mail: ornaghijr.heitor@gmail.com

F. G. Ornaghi
Postgraduate Program in Materials Science and Engineering (PGCIMAT), Federal University of Rio Grande do Sul, Av. Bento Gonçalves 9500, Porto Alegre, RS, Brazil

R. M. Neves · O. Bianchi
Postgraduate Program in Mining, Metallurgical and Materials Engineering (PPGE3M), Federal University of Rio Grande do Sul, Av. Bento Gonçalves 9500, Porto Alegre, RS, Brazil

Introduction

Lignocellulosic biomass pyrolysis has been extensively studied and it is well-known that hemicellulose primarily contributes to the thermal stability, cellulose to the Arrhenius parameters and lignin to the final “tail” of the TG curve (Yao et al. 2008; Cabeza et al. 2015; Ornaghi et al. 2019b). Hence, the thermal degradation of plant fibers is mainly dependent on the chemical composition, which is directly influenced by other factors, such as the climatic conditions. In this regard, an in-depth knowledge of the thermal behavior

of lignocellulosic biomass during pyrolysis, considering each component, is of extreme importance for the development of new and more robust model-fitting methods. Also, a good understanding of the individual and combined behavior of the different components is relevant to their use in value-added industrial applications (Li et al. 2017; Chen et al. 2016).

A knowledge of the Arrhenius parameters (activation energy and pre-exponential factor) and degradation mechanism(s) is essential for scientific studies on biomass. The use of statistical tools for determining the most probable degradation mechanism was investigated by Erceg et al. (2018). These authors evaluated the thermal degradation kinetics of poly(ethylene oxide) using a statistical tool (F-test) and found that the most probable degradation mechanism, based on Avrami-Erofeev (type-A), was a single-step process. On the other hand, Ourique et al. (2019) studied the thermo-oxidative degradation kinetics of renewable polyurethane-urea obtained from air-oxidized soybean extractives, and the main results indicated that a three-step degradation mechanism was more physically plausible than those proposed in the literature based on other methods. Ornaghi et al. (2019a) studied the thermal degradation kinetics of fluoroelastomers reinforced with carbon nanofibers. The results suggested an autocatalytic single-step degradation mechanism induced by impurities of the residual metals from the production of the carbon nanofibers, which accelerate the degradation. This was corroborated by lower E_a values being obtained for neat fluoroelastomers. Also, thermal predictions were made using different isothermal temperatures, based on the Arrhenius parameters, and the degradation mechanism from 150 to 350 °C over 105 min was investigated. The residual mass loss is easily estimated for all samples for different isotherms. Neves et al. (2019) studied the influence of silane surface modification on the characteristics of microcrystalline cellulose and, based on the degradation model proposed, the kinetics seems to follow $A \rightarrow B \rightarrow C$, regardless of the silane content. This type of study is essential because it allows model-free procedures to be developed for the reliable prediction of thermal degradation curves based on robust and reliable analysis and the verification of the consistency of the models, such as those developed by Cabeza et al. (2015) and Ali et al. (2017).

Cabeza et al. (2015) developed free spreadsheet software in which the TG curves can be estimated

from initial chemical composition data. The char formation of cellulose, hemicellulose and lignin was also evaluated as a function of temperature. Based on the software and using different heating rates, each component (water, extractives, cellulose, cellulose char, hemicellulose, hemicellulose char, lignin, and lignin char) can be individually studied without the “interference” of the others. This approach is essential because the components that have greater resistance to degradation can be used as a thermal barrier in certain polymeric materials with more thermally-labile bonds, giving more aggregated value to the final product. Ornaghi et al. (2019b) applied the F-test tool to study the degradation mechanism associated with three different lignocellulosic fibers (ramie, jute and kenaf) and the results indicated an autocatalytic reaction as the most probable degradation mechanism. The same degradation mechanism was identified by Cabeza et al. (2015) using different procedures. Ali et al. (2017) studied the application of model-free and model-fitting methods (differential and integral) to coconut shell waste in independent parallel reactions, and the results indicated that order-based nucleation and growth mechanisms control the solid-state pyrolysis. The integral method was found to be more suitable for the fitting of the experimental data at higher temperatures in comparison to the differential method. In all cases, the effect of each component is hard to separate from the others because there is an overlap in the specific temperature domain. Even for independent parallel reactions, in which each component is individually separated, the effects of the respective chars are not considered. For example, the degradation of cellulose encompasses cellulose plus cellulose char. Thus, a significant contribution to the field of study reported herein is that the Arrhenius parameters of each component present in lignocellulosic fiber (including water, extractives and the respective chars for cellulose, hemicellulose and lignin) are estimated using a specific degradation model (Waterloo’s reaction pathway) and the degradation step(s) are determined. Also, simulations of the degradation mechanisms of the individual components and of the TG curve were carried out. The procedure involved simultaneously fitting the experimental data and identifying the most common theoretical degradation mechanisms for solid-state reactions using a statistical tool (F-test). TG curves were simulated and the results discussed separately for each component. The best fit

for the total TG curve presented three degradation mechanisms which can be associated with cellulose, hemicellulose, and lignin. The char formed in the degradation plays an important role because it showed higher activation energies than the respective components. Figure 1 shows a schematic representation of the procedure.

A novel aspect of this study is the use of a statistical tool (F-test) for the determination of Arrhenius parameters and degradation mechanism for each component of the biomass fiber. The final TG curve is simulated, and the effect of each component is discussed. This robust tool offers the advantages of simultaneously fitting multiple experimental data using the selected degradation mechanisms and producing rapid results. Further details on the software are provided in the following section “Theoretical Background”. Also, the results of this study will facilitate the building of a fitting model for biomass components, by providing insights into physicochemical processes involved in the pyrolysis of the components and highlighting the degradation mechanisms associated with each component. The model developed can be used to predict the final material properties from the

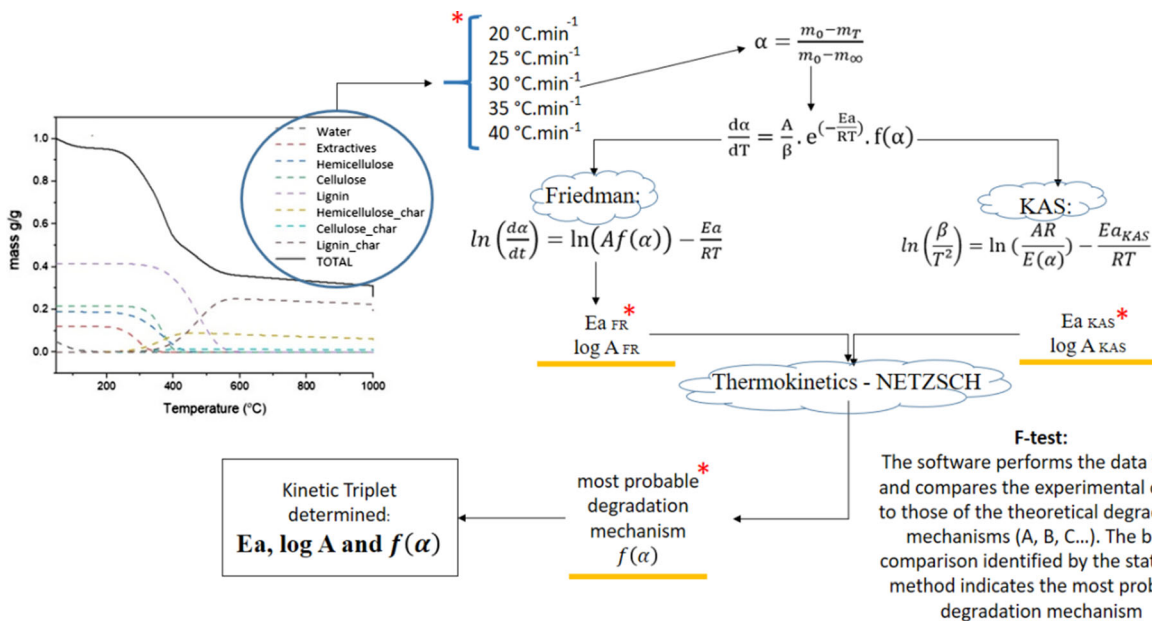
initial reactions for various biomass samples with different compositions.

Theoretical Background

According to Vyazovkin et al. (2011), the purpose of kinetic calculations is to obtain the so-called kinetic triplet, namely: (activation energy—associated with the energy barrier), (pre-exponential factor—with the frequency of vibrations of the activated complex or a “composite” effect (Ornaghi et al. 2019b)) and $f(\alpha)$ (kinetic function—reaction mechanism). These concepts were initially developed for homogeneous kinetics (e.g., metals) and later applied to materials with heterogeneous kinetic behavior, such as polymers and biomass (Galwey 1997, 2003; Boris 2001). To determine the kinetics behavior, initially, the conversion degree (α) needs to be determined. The fundamental differential equation for any kinetic study is described by Eq. (1).

$$\frac{d\alpha}{dt} = k(T) \cdot f(\alpha) \tag{1}$$

In a solid-state reaction, α , in a non-isothermal (dynamic) experiment, can be given by Eq. (2).



* For each component (water, extractives, hemicellulose, cellulose, lignin and their respective chars).

Fig. 1 Schematic representation of the procedure used to estimate the Arrhenius parameters and the most probable degradation mechanism

$$\alpha = \frac{m_0 - m_T}{m_0 - m_\infty} \quad (2)$$

As TG is a dynamic test, some adjustments have been made over years (Poletto et al. 2015) and, consequently, Eq. (3) is now used as the basis of the calculations.

$$\frac{d\alpha}{dT} = \frac{A}{\beta} \cdot e^{\left(-\frac{Ea}{RT}\right)} \cdot f(\alpha) \quad (3)$$

where m_0 is the initial weight of the sample, m_∞ is the final weight of the sample and m_T is the weight of the sample at time (t), $\frac{d\alpha}{dT}$ is the degradation rate, α is the conversion degree, T is the absolute temperature, A is the frequency factor, β is the heating rate, Ea is the activation energy, R is the gas constant, $k(T)$ is the rate constant and $f(\alpha)$ is a function of the conversion (Vyazovkin et al. 2011; Poletto et al. 2015).

There are several methods to obtain the A and Ea values and these can be found in the literature (Vyazovkin et al. 2011; Erceg et al. 2018; Friedman 1964). The Friedman (FRI) and Kissinger–Akahira–Sunose (KAS) methods were used to estimate the Arrhenius parameters. The Friedman method is a linear differential method in which, through direct relationships, $[\ln(d\alpha/dt)]$ vs. $1/T$ results in a slope value for $(-Ea_{FR}/R)$ and the intercept for A (Friedman 1964). FRI method is described by Eq. (4).

$$\ln\left(\frac{d\alpha}{dt}\right) = \ln(Af(\alpha)) - \frac{Ea_{FR}}{RT} \quad (4)$$

Conversely, the Kissinger–Akahira–Sunose method (KAS) is an integral linear differential, in which, by linear regression, β/T^2 vs. $1/T$ results in a slope value that provides values for the activation energy (Vyazovkin et al. 2011). The KAS method is described by Eq. (5).

$$\ln\left(\frac{\beta}{T^2}\right) = \ln\left(\frac{AR}{g(\alpha)Ea_{KAS}}\right) - \frac{Ea_{KAS}}{RT} \quad (5)$$

Lastly, from the A and Ea values it is possible to obtain the most probable degradation mechanism. This last part of the kinetic triplet was selected based on F -statistic tests by simultaneously fitting all experimental and theoretical curves. The theoretical models can be selected from a variety of numerical and graphical methods from Netzsch software (Ali et al. 2017; Erceg et al. 2018). This software can analyze a dataset containing the relevant dynamic and/or isothermal

measurements. It is also possible to use model-free and model-based approaches. The model-free methods are widely used but they only find activation energy of a process without any parallel or competitive steps, and then make predictions. However, they can not provide information on the number of steps, their contribution to the total effect of reaction or the reaction order for each step. Model-based analysis is based on assumptions regarding the kinetic model of the process, uses powerful mathematics to solve the system of differential equations and makes a statistical comparison of the models used and therefore can answer all of these questions. Model-free analysis involves the evaluation methods described in ASTM e698, Friedman analysis, KAS and FWO analysis. Model-based kinetic analysis can be used based on models that include processes of up to six-steps and in which the individual steps are independent, parallel, competing and so on. All unknown parameters (activation energy, pre-exponential factor, reaction order, autocatalysis order (for autocatalytic reactions)) will be found from the fitting of measured data with the simulated curves for the given reaction types. Statistical comparison of the fits for different models allows the appropriate model, with the corresponding set of parameters, to be selected. Poletto et al. (2015) schematically represented the most common degradation mechanisms found in the literature. They are well described in the literature and the most common are type-A (nucleation and nuclei growth models), type-R (geometrical contraction models), type-D (diffusion models), type-F (order-based models) and types-B and C (autocatalytic models). The type-A (Avrami–Erofeev) model considers that: i) ingestion (elimination of a potential nucleation site and growth of an existing nucleus), and ii) coalescence (loss of reactant/product interface when reaction zones of two or more growing nuclei merge) are both responsible for the restrictions imposed on nuclei growth. These restrictions play a significant role in the solid-state decomposition. Autocatalytic models (types-B and -C) occur if the growth of nuclei promotes continued reaction due to the formation of imperfections (e.g., when the reactants are regenerated during a reaction, catalyzing the reaction). The termination of the reaction occurs when the reaction begins to spread into the material that has decomposed. In the case of geometrical contraction (type-R) models, it is assumed that nucleation occurs rapidly on the surface of the crystal and the rate of

degradation is controlled by the resulting reaction interface progressing toward the center of the crystal. Depending on the crystal shape, different mathematical models can be derived, such as contracting cylinder (contracting area) or contracting sphere/cube (contracting volume). Diffusion (type-D) models assume that a solid-state reaction occurs between crystal lattices or with molecules that permeate the lattice defects. Order-based models (type-F) assume that the reaction rate is proportional to the concentration, amount or fraction remaining of reactant raised to a particular power (integral or fractional), which is the reaction order (Khawam and Flanagan 2006).

Materials and methods

The study was divided into two distinct parts:

- i. Theoretical study based on the Cabeza spreadsheet in an Excel file (Cabeza et al. 2015). We used the raw data from TG curves (for kenaf fiber) and simulated them with the following heating rates: 5, 10, 15, 20, 25, 30, 35, and 40 °C min⁻¹. The degradation curves were then separated from the main chemical components presented: water, extractives, hemicellulose, cellulose, lignin, and their respective chars. The program developed (Biomass Modelling—Thermal degradation) is available free of charge on the web: <http://hpp.uva.es/software/>.
- ii. The aforementioned chemical components were separately simulated applying the following heating rates: 20, 25, 30, 35 and 40 °C min⁻¹. The *Ea* and *A* values were then obtained using the Friedman and KAS methods (described in the previous section). Lastly, the degradation model and the most probable degradation mechanism(s) were statistically evaluated based on the dependence of the activation energy on the conversion degree. The statistical analysis was carried out using the F-statistic tool in the Netzsch software.

Results and discussion

Previous studies (Cabeza et al. 2015; Ornaighi et al. 2019b) have shown that both diffusion and

autocatalysis are the most probable degradation mechanisms governing the thermal degradation of lignocellulosic materials. Cellulose is principally responsible for the Arrhenius parameters (activation energy and pre-exponential factor) while hemicellulose is associated with the reaction order (Sunphorka et al. 2017). The major contribution of lignin is the “tail” in the last main degradation step. In biomass, lignin does not influence the kinetic parameters. A fiber with an initial composition (g/g) of 22.9% cellulose (C), 18.8% hemicellulose (HC), 41.6% lignin (L), 4.7% water (W) and 12.0% extractives (E) was simulated at different heating rates in order to calculate the following kinetic parameters: activation energy (*Ea*), pre-exponential factor (*A*) and the most probable degradation mechanism(s). The *dT/dt* initially established by Cabeza et al. (2015) was used. Figure 2a shows the thermogravimetric curves at different heating rates. At heating rates lower than 20 °C min⁻¹ the curve did not extend to 1000 °C, so these results were not used in the subsequent calculations. Figure 2b shows the representative curve for 35 °C min⁻¹, in which the TG curve for each component is shown. Also, the char formation with temperature is presented for lignin (LC), hemicellulose (HCC) and cellulose (CC). Each thermal degradation curve of the components (L, H, HC, LC, HCC, CC) was obtained at different heating rates. Similar curves were noted for all curves at different heating rates, but the main events showed a shift with the heating rate (heat transfer effect).

Cabeza's approach is very attractive and has made an immense contribution to the scientific field because it allows the effect of each component to be observed on the TG curve. Also, the evolution of char with temperature shows that the degradation involves multiple degradation steps, which makes the modeling very complex. Waterloo's degradation model, in which all solids decompose into volatiles and char, seems to be the most suitable model to describe the degradation behavior of lignocellulosic fibers. The autocatalytic degradation mechanism proposed by Cabeza et al. (2015) is based on the cleavage of cellulosic materials, leading to the production of oligomers, which further accelerate the depolymerization. Based on this model, Ornaighi et al. (2019b) simulated the thermal behavior of different types of biomass applying the F-test method and using the models most commonly found in the literature. The

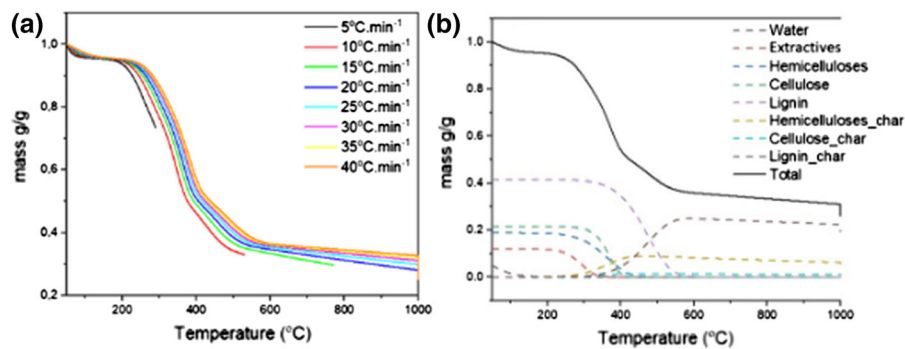


Fig. 2 a Simulated total curves using heating rates from 5 to 40 °C in steps of 5 °C and b) representative curve simulated with a heating rate of 35 °C min⁻¹. At heating rates from 5 to

theoretical data was simultaneously compared with experimental curves obtained at different heating rates. The degradation mechanism observed by the authors was autocatalysis.

Thermal degradation has been extensively described. At ca. 100 °C there is the elimination of water, which is corroborated by the water curve (dotted black line). The amount of water present in lignocellulosic fiber is dependent on the humidity, and it should be noted that the mass loss is due to water evaporation or, in some cases, sublimation of components of low molecular weight (Yao et al. 2008; Ornaghi et al. 2016). Water loss represents ca. 5 wt % of the total mass loss and can accelerate the degradation leading to decreased thermal stability. The calculation of the TG curves was considered from 100 °C (hence, it did not account for water evaporation) to ensure that the main degradation range was consistent with those reported in the literature (Yao et al. 2008; Ali et al. 2017). According to reports in the literature, hemicellulose is mainly responsible for the thermal stability and reaction order (Sunphorka et al. 2017; Ornaghi et al. 2019b), cellulose for the degradation and for the Arrhenius parameters (Sunphorka et al. 2017; Ornaghi et al. 2019b), and lignin for the final “tail” of TG curve (Yao et al. 2008; Poletto et al. 2015).

Figure 3 shows the TG curves for the cellulose, hemicellulose and lignin components along with respective chemical structures. This figure allows a comparison of the effect of each component on the degradation. The effect of the three major contributors is highlighted. In the biomass structure, cellulose microfibrils are connected by hemicellulose in the 3D

structure of the lignin that surrounds and protects them. Lignin can be described as a complex, cross-linked, three-dimensional aromatic polymer comprised of phenylpropane units, and its degradation occurs at a higher temperature compared to the other components. Hemicellulose and cellulose are made up of monomeric sugars. The difference between them is that cellulose is a linear polymer made up of anhydroglucopyranose (hexose) units linked by ether bonds, while hemicellulose is a branched and amorphous polymer formed of both pentoses and hexoses (Faruk et al. 2012; Azwa et al. 2013).

There are conflicting reports in the literature in relation to the possibility that interactions between the cellulose, hemicellulose, and lignin products formed during pyrolysis lead to different final chemical

structure of the lignin that surrounds and protects them. Lignin can be described as a complex, cross-linked, three-dimensional aromatic polymer comprised of phenylpropane units, and its degradation occurs at a higher temperature compared to the other components. Hemicellulose and cellulose are made up of monomeric sugars. The difference between them is that cellulose is a linear polymer made up of anhydroglucopyranose (hexose) units linked by ether bonds, while hemicellulose is a branched and amorphous polymer formed of both pentoses and hexoses (Faruk et al. 2012; Azwa et al. 2013).

There are conflicting reports in the literature in relation to the possibility that interactions between the cellulose, hemicellulose, and lignin products formed during pyrolysis lead to different final chemical

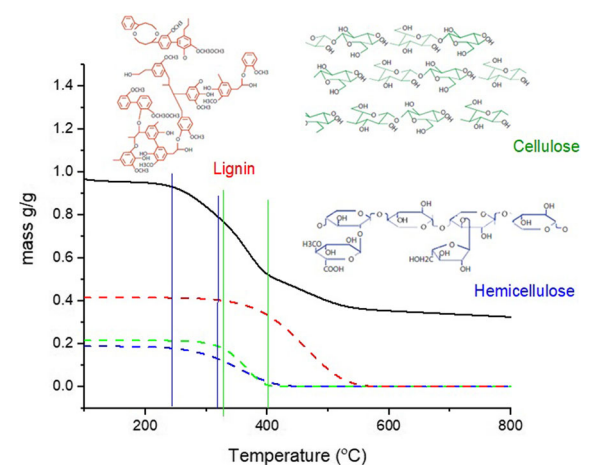


Fig. 3 Thermogravimetric curves showing the individual components lignin, cellulose and hemicellulose with their respective chemical structures

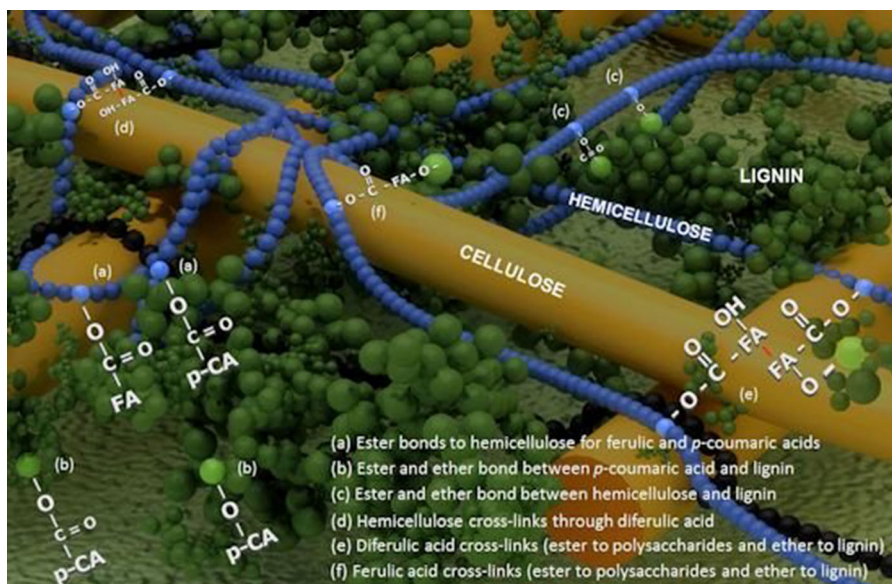


Fig. 4 Representation of the physical structure of biomass showing the respective chemical bonds [figure taken from Santiago et al. 2013]

distributions. Some authors propose negligible interactions among the components during pyrolysis, while other researchers have reported their importance. The influence of inorganic salts on the primary pyrolysis products of cellulose was studied by Patwardhan (2010). These authors stated that inorganic salts and ash act (with temperature) as a catalyst via competitive reactions, accelerating the reaction and leading to the formation of low molecular weight species from cellulose. The cited authors determined the distribution of low molecular weight species (formic acid, glucoaldehyde and acetol), furan ring derivatives (2-furaldehyde and 5-hydroxymethyl furfural), and anhydro sugars (levoglucosan). Patwardhan et al. 2011 studied the distribution of the products from the rapid pyrolysis of hemicellulose and observed that the behavior differed considerably from that of cellulose, which was attributed to glycosidic bond cleavage. In another study (Patwardhan et al. 2011b), 24 primary products from corn stover lignin pyrolysis were reported, most of them resulting in the formation of monomeric phenolic compounds as the major products. All of the aforementioned studies led to the proposal of a specific reaction scheme/mechanism.

Zhang et al. (2015) studied the binary interactions of cellulose-hemicellulose and cellulose-lignin for woody (industrial wood chips, sawdust, waste wood)

and herbaceous (straw, cereals, grasses) biomass. The hemicellulose-lignin binary system was not included in their study due to the difficulty in obtaining it. In the case of a cellulose-lignin mixture, the herbaceous biomass exhibited an apparent interaction, represented by a decrease in the amount of levoglucosan and an increase in the amount of low molecular weight compounds and furans. This interaction was not observed for woody biomass. The authors speculated that there may be different amounts of covalent linkages in this biomass. Figure 4 shows a representation of the physical structure, as well as the chemical bonds between the biomass components. By observing the complexity of the biomass composition, it seems plausible that the pyrolytic behavior cannot be easily captured by the simple addition of the individual components. The reactive species that may be released during the rapid pyrolysis of individual biopolymers can interact differently. Thus, the product distribution would not be the same as a simple overlap of the pyrolysis products of the individual components.

Figures 5 a-h show the simulations for the individual components carried out to determine the degradation mechanisms and Arrhenius parameters (given in Table 1). Water was considered to have a degradation mechanism in this case for comparison (it evaporates with temperature but has a specific activation energy).

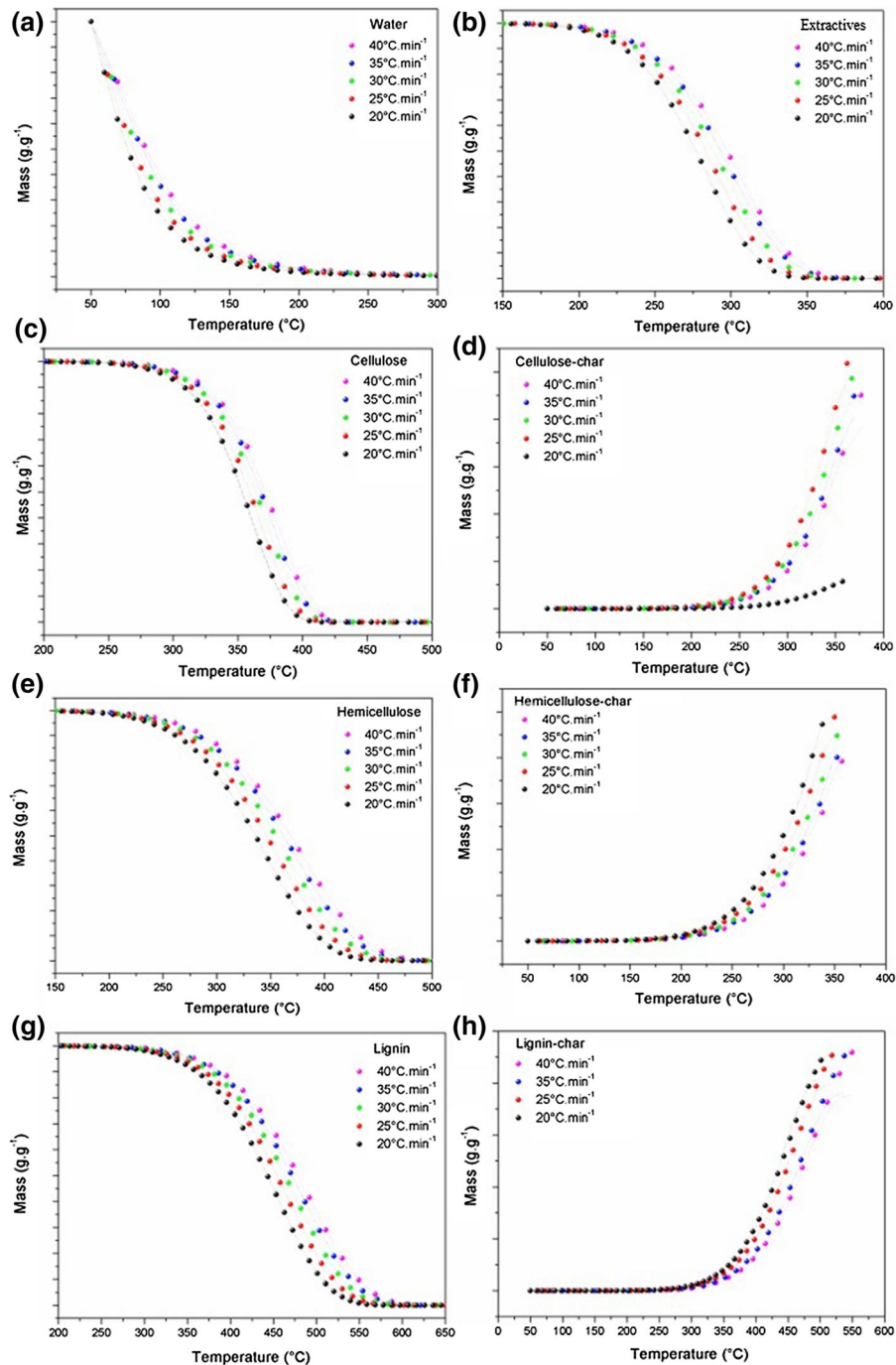


Fig. 5 Experimental and simulated data for **a** water, **b** extractives, **c** cellulose, **d** cellulose char, **e** hemicellulose, **f** hemicellulose char, **g** lignin and **h**) lignin char

All degradation models followed $A \rightarrow B$, i.e., a one-step degradation mechanism. All R^2 values were above 0.99. Table 1 shows the ten best fits for all components. The one-step mechanism does not

necessarily represent a single reaction; it could be the sum of parallel/consecutive reactions as well as a single dependence of E_a on the conversion degree (Moukhina, 2012; Ornaghi et al. 2019a; Ourique et al.

Table 1 Results obtained with F-test statistical tool for all individual biomass components tested

Sample	Mechanism $f(\alpha)$	E_a (kJ mol ⁻¹)	$\text{Log } A$ (s ⁻¹)	F_{exp}	R^2	Extractives	Mechanism $f(\alpha)$	E_a (kJ mol ⁻¹)	$\text{Log } A$ (s ⁻¹)	F_{exp}	R^2		
Water	C _n	35.08	5.29	1.00	0.9999	Extractives	B _n	79.67	7.29	1.00	0.9999		
	B _n	35.35	5.40	2.02	0.9999		C _n	81.78	7.45	1.97	0.9999		
	F _n	37.28	5.66	5.17	0.9999		F _n	82.38	7.52	2.03	0.9999		
	F ₂	35.02	5.30	6.56	0.9999		A _n	79.74	7.25	3.59	0.9999		
	A _n	17.99	2.49	451.08	0.9966		F ₁	80.44	7.32	3.60	0.9999		
	F ₁	8.77	1.12	577.40	0.9956		C ₁	80.44	7.32	3.65	0.9999		
	C ₁	8.77	1.12	580.46	0.9956		R ₃	70.30	5.78	81.47	0.9993		
	D ₃	32.60	3.54	1069.24	0.9919		R ₂	65.76	5.48	167.19	0.9985		
	R ₃	1.96	-0.46	1305.59	0.9901		D ₃	142.3	12.09	212.68	0.9982		
	D ₄	24.83	2.29	1357.84	0.9897		F ₂	118.99	11.30	273.91	0.9977		
	Cellulose	C _n	118.32	9.58	1.00		0.9999	Cellulose	D ₂	157.78	13.13	1.00	0.9999
		F _n	119.01	9.65	1.03		0.9999		D ₄	165.46	13.21	4.58	0.9998
		B _n	119.04	9.65	1.05		0.9999		D ₁	138.30	11.57	14.65	0.9995
		C ₁	117.57	9.51	1.28		0.9999		D ₃	179.99	14.60	20.32	0.9993
A _n		120.85	9.82	2.87	0.9999	A _n	166.11		14.48	54.25	0.9982		
F ₁		122.87	9.99	2.97	0.9999	R ₃	88.15		6.99	74.17	0.9975		
R ₃		107.73	8.15	22.12	0.9997	F _n	89.71		7.61	74.78	0.9975		
R ₂		101.26	7.74	60.27	0.9992	C _n	89.70		7.62	75.78	0.9975		
D ₃		215.49	16.61	105.86	0.9986	B _n	90.80		7.72	75.92	0.9975		
D ₄		195.15	14.81	126.65	0.9984	R ₂	82.96		6.66	81.69	0.9973		
Hemicellulose		B _n	58.99	4.56	1.00	0.9999	Hemicellulose		D ₁	111.19	9.40	1.00	0.9990
		C ₁	59.02	4.53	1.20	0.9999			D ₂	125.54	10.55	1.32	0.9988
		A _n	59.42	4.59	1.47	0.9999			D ₄	132.21	10.56	1.90	0.9982
		C _n	58.86	4.51	2.32	0.9999			R ₂	67.86	5.42	1.92	0.9982
	F _n	59.63	4.60	2.44	0.9999	F _n		68.54	5.79	1.94	0.9982		
	F ₁	60.50	4.68	3.84	0.9999	C _n		68.54	5.79	1.96	0.9982		
	R ₃	52.36	3.40	572.95	0.9995	B _n		65.43	5.48	2.07	0.9981		
	R ₂	48.88	3.23	1379.60	0.9989	R ₃		72.00	5.67	2.08	0.9980		
	D ₃	108.51	7.69	2025.88	0.9983	C ₁		72.68	6.20	3.04	0.9972		
	D ₄	97.69	6.66	2546.35	0.9979	D ₃		144.50	11.78	3.32	0.9969		

Table 1 continued

Sample	Mechanism $f(\alpha)$	E_a (kJ mol ⁻¹)	$\text{Log } A$ (s ⁻¹)	F_{exp}	R^2	Mechanism $f(\alpha)$	E_a (kJ mol ⁻¹)	$\text{Log } A$ (s ⁻¹)	F_{exp}	R^2
Lignin	B _n	75.41	4.95	1.00	0.9999	Lignin	80.79	5.49	1.00	0.9990
	F _n	75.57	4.96	1.06	0.9999	char	79.39	4.89	1.01	0.9990
	F ₁	76.23	5.01	1.42	0.9999	C _n	80.79	5.49	1.01	0.9990
	A _n	75.40	4.95	2.20	0.9999	B _n	80.20	5.44	1.02	0.9990
	C _n	74.79	4.89	2.78	0.9999	D ₂	136.33	9.13	1.34	0.9987
	C ₁	74.73	4.89	2.89	0.9999	R ₂	74.43	4.64	1.41	0.9986
	R ₃	66.02	3.69	748.57	0.9995	C ₁	84.66	5.81	1.42	0.9986
	R ₂	61.4	3.49	1751.26	0.9988	D ₄	144.51	9.14	1.43	0.9986
	D ₃	13.13	8.28	2404.40	0.9984	A _n	97.04	6.80	1.45	0.9986
	D ₄	123.07	7.22	3057.81	0.9980	F ₁	89.67	6.24	1.51	0.9985

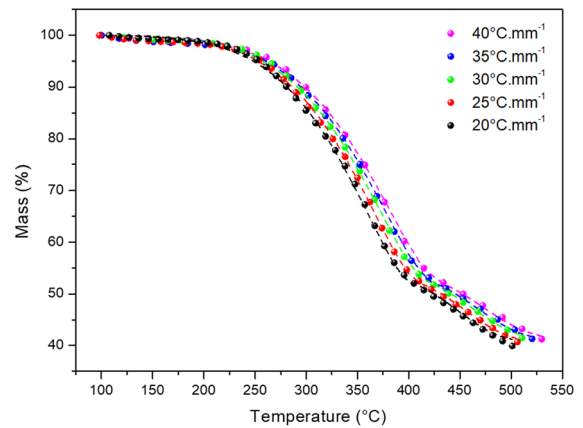


Fig. 6 Simulated and theoretical TG curves for different heating rates

2019; Zanchet et al. 2019). This is more likely in composite systems, such as biomass plant fibers, and has been reported in the literature (Yao et al. 2008). Therefore, it will be considered that parallel/consecutive reactions are not occurring for each component. The experimental values of the F -test obtained for each component were: water F_{test} 1.27, extractives F_{test} 1.45, hemicellulose F_{test} 1.34, hemicellulose char F_{test} 1.43, cellulose F_{test} 1.45, cellulose char F_{test} 1.46, lignin F_{test} 1.32 and lignin char F_{test} 1.43. The values below are considered statistically significant, indicating the most probable degradation mechanisms.

The most extensive temperature range of thermal degradation was observed for the aromatic components of lignin. Lignin is expected to have a lower activation energy as it is an amorphous component. Cellulose is crystalline and the crystals act as a thermal barrier that inhibits the heat transfer. Thus, a greater amount of energy is required for the molecular motion, increasing the activation energy, which is higher for cellulose than hemicellulose. For lignin, the formation of char also extends across a wider temperature range when compared to the cellulosic components.

The TG curve from 100 to 550 °C was simulated (Fig. 6) and the degradation mechanism was calculated, thus the Arrhenius parameters and degradation mechanisms were found for each individual component. The total curve was simulated based on the best recently published degradation models (Yao et al. 2008). The best fit for all of the different steps is shown in Fig. 6. One, two and three steps were considered to perform a complete statistical evaluation. The results

Table 2 The most probable degradation mechanisms for the TG curve

Sample	Mechanism $f(\alpha)$	$Ea(\text{kJ mol}^{-1})$	$\text{Log } A (\text{s}^{-1})$	F_{exp}	R^2
Total curve	D ₄	96.39	4.99	1.00	0.9997
	C _n	111.00	5.96		
	C _n	111.00	11.00		0.9997
	D ₃	104.99	5.80	1.17	
	C _n	111.00	5.79		0.9996
	C _n	111.00	11.00		
	C _n	74.88	4.12	2.01	0.9993
	C _n	100.00	11.00		
	C _n	24.44	3.13		0.9989
	C _n	74.47	4.22	3.36	
	C _n	100.00	11.00		0.9987
	C _n	26.45	3.31		
	C _n	57.88	2.38	5.44	0.9986
	C _n	100.00	11.00		
	C _n	62.30	3.05	5.62	0.9984
	F _n	69.31	3.80	6.33	
	D ₃	93.26	4.59	6.40	0.9983
	C _n	111.00	4.75		
	C _n	111.00	11.00		0.9983
	D ₂	55.18	1.86	8.27	
C _n	111.00	8.10		0.9983	
C _n	111.00	11.00			

$$F_{\text{test}}^2 = 1.32$$

showed that the activation energy is dependent on cellulose, while hemicellulose plays a significant role in the reaction order. These results corroborate the findings of previous studies conducted using statistical and integral methods and artificial neural networks (Sunphorka et al. 2017; Ormaghi et al. 2019b).

Table 2 shows all of the conditions tested. The activation energies are lower for hemicellulose and cellulose and higher for lignin compared to data published in the literature. Yao et al. 2008 reported values of 105–111 kJ mol⁻¹ for hemicellulose, 195–213 kJ mol⁻¹ for cellulose and 36–65 kJ mol⁻¹ for lignin. These differences could be because in all of the studies reported in the literature the chars formed in each degradation were not separated. Chars have higher Ea values than the respective components. Water, extractives, cellulose, hemicellulose and lignin presented, in general, autocatalysis as the most probable degradation mechanism (C_n or B_n). Cellulose and hemicellulose chars presented a diffusion-type (D-

type) mechanism while lignin shows a more complex mechanism, presenting random nucleation (F-type), geometrical contraction (R-type), autocatalysis (Bn-type) and diffusion (D-type). Lignin is the most complex material in biomass and it seems plausible that its char has a wide range of degradation mechanisms. This highlights the challenge associated with modelling in the final degradation stage, i.e., the degradation of all the main components and their chars needs to be considered, and some of them have different degradation mechanisms. The autocatalytic mechanisms presented for most of the materials also seem physically plausible, since the chain cleavage produces oligomers that accelerate further depolymerization. Lignin (79.1–226.5 kJ mol⁻¹) and cellulose (106.4 kJ mol⁻¹) had values similar to those obtained by Ali et al. (2017) using a different model-fitting procedure. The same procedure provided higher hemicellulose values (108.6 kJ mol⁻¹).

The most probable degradation mechanism found was diffusion, followed by autocatalysis. This result suggests that hemicellulose char and cellulose char could be responsible for the diffusion mechanism in the first thermal degradation step. The results obtained by Ornaghi (2019b) for kenaf, jute, and ramie showed three autocatalytic mechanisms as the most probable degradation mechanism. But diffusion followed by two consecutive autocatalytic processes was the second most probable degradation mechanism. These differences can be attributed to the chemical composition. Higher hemicellulose and cellulose contents lead to a greater amount of char being produced and this can play an important role in the diffusion mechanism of the first step.

The individual Arrhenius values found cannot be attributed to the main components (i.e., the first to hemicellulose, the second to cellulose and the third to lignin). Thermal degradation is very complex and thus it is expected that the Arrhenius values will not always be the same for the individual components. The char formation also contributes significantly to the degradation. Thus, the three degradation mechanisms seem to refer to the three main components, while the Arrhenius values obtained for the process do not.

Conclusions

This study focused on the degradation mechanism of each component of lignocellulose biomass fiber (water, extractives, cellulose, hemicellulose, lignin, cellulose char, hemicellulose char and lignin char), applying the F-test tool and simulating each component separately. One, two and three steps were considered to complete the statistical evaluation during the simulation. The results for the activation energy showed a dependence on cellulose and the reaction order was associated with hemicellulose. Since lignin is the most complex material in biomass, a wide range of degradation mechanisms are associated with the respective char. This study demonstrates the implementation of more robust integral fitting models, considering the effect of each component. The models indicated that the degradation mechanism that most occurred in the biomass was diffusion, followed by autocatalysis. Higher levels of cellulose and hemicellulose lead to a great amount of their chars, which play a significant role in the first step of the thermal

diffusion mechanism. The results reported herein could be used for the development of new fitting models with well-defined reaction steps. Water presented a lower E_a (35 kJ mol^{-1}) in comparison to hemicellulose (50 kJ mol^{-1}), cellulose (118 kJ mol^{-1}) and lignin (75 kJ mol^{-1}). The char of the main lignocellulosic components showed higher activation energies (cellulose: 157 kJ mol^{-1} , hemicellulose 110 kJ mol^{-1} , and lignin 80 kJ mol^{-1}) compared to the respective components. However, the TG curve showed an average of 111 kJ mol^{-1} , separated into three distinct degradation steps.

Acknowledgments This study was financed in part by the Coordenação de Aperfeiçoamento de Pessoal de Nível Superior—Brasil (CAPES)—Finance Code 001. The authors also acknowledge CNPq (Process number: 153335/2018-1).

References

- Ali I, Bahaitham H, Naibulharam R (2017) A comprehensive kinetics study of coconut shell waste pyrolysis. *Bioresour Technol* 235:1–11. <https://doi.org/10.1016/j.biortech.2017.03.089>
- Azwa ZN, Yousif BF, Manalo AC, Karunasena W (2013) A review on the degradability of polymeric composites based on natural fibres. *Mater Des* 47:424–442. <https://doi.org/10.1016/j.matdes.2012.11.025>
- Boris VL (2001) The physical approach to the interpretation of the kinetics and mechanisms of thermal decomposition of solids: the state of the art. *Thermochim Acta* 373:97–124
- Cabeza A, Sobrón F, Yedro FM, García-Serna J (2015) Auto-catalytic kinetic model for thermogravimetric analysis and composition estimation of biomass and polymeric fractions. *Fuel* 148:212–225. <https://doi.org/10.1016/j.fuel.2015.01.048>
- Chen GG, Qi XM, Guan Y et al (2016) High Strength Hemicellulose-Based Nanocomposite Film for Food Packaging Applications. *ACS Sustain Chem Eng* 4:1985–1993. <https://doi.org/10.1021/acssuschemeng.5b01252>
- Erceg M, Krešić I, Vrandečić NS, Jakić M (2018) Different approaches to the kinetic analysis of thermal degradation of poly(ethylene oxide). *J Therm Anal Calorim* 131:325–334. <https://doi.org/10.1007/s10973-017-6349-6>
- Faruk O, Bledzki AK, Fink HP, Sain M (2012) Biocomposites reinforced with natural fibers: 2000–2010. *Prog Polym Sci* 37:1552–1596. <https://doi.org/10.1016/j.progpolymsci.2012.04.003>
- Friedman HL (1964) Kinetics of thermal degradation of char-forming plastics from thermogravimetry. Application to a phenolic plastic. *J Polym Sci Part C Polym Symp* 6:183–195. <https://doi.org/10.1002/polc.5070060121>
- Galwey AK (1997) Compensation behaviour recognized in literature reports of selected heterogeneous catalytic reactions: aspects of the comparative analyses and significance

- of published kinetic data. *Thermochim Acta* 294:205–219. [https://doi.org/10.1016/S0040-6031\(96\)03153-X](https://doi.org/10.1016/S0040-6031(96)03153-X)
- Galwey AK (2003) Eradicating erroneous Arrhenius arithmetic. *Thermochim Acta* 399:1–29. [https://doi.org/10.1016/S0040-6031\(02\)00465-3](https://doi.org/10.1016/S0040-6031(02)00465-3)
- Khawam A, Flanagan DR (2006) Solid-state kinetic models: basics and mathematical fundamentals. *J Phys Chem B* 110:17315–17328. <https://doi.org/10.1021/jp062746a>
- Li H, Sun JT, Wang C et al (2017) High Modulus, Strength, and Toughness Polyurethane Elastomer Based on Unmodified Lignin. *ACS Sustain Chem Eng* 5:7942–7949. <https://doi.org/10.1021/acssuschemeng.7b01481>
- Moukhina E (2012) Determination of kinetic mechanisms for reactions measured with thermoanalytical instruments. *J Therm Anal Calorim* 109:1203–1214. <https://doi.org/10.1007/s10973-012-2406-3>
- Neves RM, Ornaghi HL, Zattera AJ, Amico SC (2019) The influence of silane surface modification on microcrystalline cellulose characteristics. *Carbohydr Polym*. <https://doi.org/10.1016/j.eplepsyres.2019.106192>
- Ornaghi HL, de Moraes AG, de O Poletto M et al (2016) Chemical composition, tensile properties and structural characterization of buriti fiber. *Cell Chem Technol* 50:15–22
- Ornaghi FG, Bianchi O, Ornaghi HL, Jacobi MAM (2019a) Fluoroelastomers reinforced with carbon nanofibers: a survey on rheological, swelling, mechanical, morphological, and prediction of the thermal degradation kinetic behavior. *Polym Eng Sci* 59:1223–1232. <https://doi.org/10.1002/pen.25105>
- Ornaghi HL, Ornaghi FG, de Carvalho Benini KCC, Bianchi O (2019b) A comprehensive kinetic simulation of different types of plant fibers: autocatalytic degradation mechanism. *Cellulose* 0123456789:7145–7157. <https://doi.org/10.1007/s10570-019-02610-x>
- Ourique PA, Ornaghi FG, Ornaghi HL et al (2019) Thermo-oxidative degradation kinetics of renewable hybrid polyurethane–urea obtained from air-oxidized soybean oil. *J Therm Anal Calorim* 9:1–11. <https://doi.org/10.1007/s10973-019-08089-9>
- Patwardhan PR, Satrio JA, Brown RC, Shanks BH (2010) Influence of inorganic salts on the primary pyrolysis products of cellulose. *Bioresour Technol* 101:4646–4655. <https://doi.org/10.1016/j.biortech.2010.01.112>
- Patwardhan PR, Brown RC, Shanks BH (2011a) Product distribution from the fast pyrolysis of hemicellulose. *ChemSuschem* 4:636–643. <https://doi.org/10.1002/cssc.201000425>
- Patwardhan PR, Brown RC, Shanks BH (2011b) Understanding the fast pyrolysis of lignin. *ChemSuschem* 4:1629–1636. <https://doi.org/10.1002/cssc.201100133>
- Poletto M, Ornaghi Jnior HL, Zattera AJ (2015) Thermal Decomposition of Natural Fibers: kinetics and Degradation Mechanisms. *React Mech Therm Anal Adv Mater* 21:515–545. <https://doi.org/10.1002/9781119117711.ch21>
- Santiago R, Barros-Rios J, Malvar RA (2013) Impact of cell wall composition on maize resistance to pests and diseases. *Int J Mol Sci* 14:6960–6980. <https://doi.org/10.3390/ijms14046960>
- Sunphorka S, Chalermssinsuwan B, Piumsomboon P (2017) Artificial neural network model for the prediction of kinetic parameters of biomass pyrolysis from its constituents. *Fuel* 193:142–158. <https://doi.org/10.1016/j.fuel.2016.12.046>
- Vyazovkin S, Burnham AK, Criado JM et al (2011) ICTAC Kinetics Committee recommendations for performing kinetic computations on thermal analysis data. *Thermochim Acta* 520:1–19. <https://doi.org/10.1016/j.tca.2011.03.034>
- Yao F, Wu Q, Lei Y et al (2008) Thermal decomposition kinetics of natural fibers: activation energy with dynamic thermogravimetric analysis. *Polym Degrad Stab* 93:90–98. <https://doi.org/10.1016/j.polymdegradstab.2007.10.012>
- Zanchet A, Demori R, de Sousa FDB et al (2019) Sugar cane as an alternative green activator to conventional vulcanization additives in natural rubber compounds: thermal degradation study. *J Clean Prod* 207:248–260. <https://doi.org/10.1016/j.jclepro.2018.09.203>
- Zhang J, Choi YS, Yoo CG et al (2015) Cellulose-hemicellulose and cellulose-lignin interactions during fast pyrolysis. *ACS Sustain Chem Eng* 3:293–301. <https://doi.org/10.1021/sc500664h>

Publisher's Note Springer Nature remains neutral with regard to jurisdictional claims in published maps and institutional affiliations.